Enhanced CRAd Activity Using Enhancer Motifs Driven by a Nucleosome Positioning Sequence

Soraya Bravo[1], Felipe Núñez[2], Fernando Cruzat[3], Eduardo G Cafferata[2], Giancarlo V De Ferrari[1], Martín Montecino[1] and Osvaldo L Podhajcer[2]

[1]Centro de Investigaciones Biomédicas and FONDAP Center for Genome Regulation, Universidad Andres Bello, Santiago, Chile; [2]Fundación Instituto Leloir, IIBBA-CONICET, Buenos Aires, Argentina; [3]Facultad de Ciencias Biológicas, Universidad de Concepción, Concepción, Chile

Cancer development involves changes driven by the epigenetic machinery, including nucleosome positioning. Recently, the concept that adenoviral replication may be driven by tumor specific promoters (TSPs) gained support, and several conditionally replicative adenoviruses (CRAd) exhibited therapeutic efficacy in clinical trials. Here, we show for the first time that placing a nucleosome positioning sequence (NPS) upstream of a TSP combined with Wnt-responsive motifs (pART enhancer) enhanced the TSP transcriptional activity and increased the lytic activity of a CRAd. pART enhanced the transcriptional activity of the gastrointestinal cancer (GIC)-specific REG1A promoter (REG1A-pr); moreover, pART also increased the *in vitro* lytic activity of a CRAd whose replication was driven by REG1A-Pr. The pART enhancer effect *in vitro* and *in vivo* was strictly dependent on the presence of the NPS. Indeed, deletion of the NPS was strongly deleterious for the *in vivo* antitumor efficacy of the CRAd on orthotopically established pancreatic xenografts. pART also enhanced the specific activity of other heterologous promoters; moreover, the NPS was also able to enhance the responsiveness of hypoxia- and NFκB-response elements. We conclude that NPS could be useful for gene therapy approaches in cancer as well as other diseases.

Received 4 December 2012; accepted 10 April 2013; advance online publication 28 May 2013. doi:10.1038/mt.2013.93

INTRODUCTION

Cancer is the second leading cause of death in the developed world,[1,2] and gastrointestinal cancers (GICs) are among the most frequently occurring cancers worldwide.[3] Gastric cancer is the fourth most common cancer among GICs worldwide, accounting for >10% of cancer-related deaths. In most cases, patients are diagnosed at an advanced stage of the disease and have an estimated 5-year survival rate of <20%.[1,2,4] Pancreatic cancer ranks as the fourth and fifth common cancer in men and women, respectively, and has the lowest 5-year survival rate of any GIC. Due to the absence of effective screening methods, pancreatic cancer is often diagnosed at advanced stages.[5] Finally, colorectal cancer is the third most common cancer globally and has the fourth highest mortality rate, accounting for almost 8% of all cancer-related deaths.[2–4]

Despite advances in the use of diagnostic imaging, such as endoscopy or colonoscopy for improved early detection, certain GICs, such as pancreatic and gastric cancers, and advanced stages of colon cancer are not amenable to current mainstay treatments.[6] Personalized medicine has improved the response in patients with advanced colorectal cancer treated with the EGFR-targeted antibody cetuximab and in gastric cancer patients expressing the erbB receptor treated with trastuzumab.[7] However, only a small percentage of patients with gastric and colorectal cancers can benefit from novel therapies, and in all cases, the benefit is mainly transient due to tumor heterogeneity. In pancreatic cancer, standard and novel therapies have failed to attenuate disease aggressiveness or confer improvements in survival.[6] Thus, novel therapies are urgently needed.

Adenovirus-based virotherapy appears as a novel approach for the treatment of different types of cancer including those of gastrointestinal origin.[8] These oncolytic adenoviruses have been introduced to target GICs, and a few have been rapidly translated to the clinic, where their safety has been clearly demonstrated.[9] However, despite their promise in preclinical trials and the safety observed in humans, oncolytic adenoviruses have shown limited efficacy in clinical trials thus far.[9,10] For instance, ONYX-15, a naturally occurring E1B-deleted replicating oncolytic adenovirus, has been used in clinical trials for advanced colorectal cancer,[11] GICs metastatic to the liver[12] and locally advanced pancreatic cancer[13,14] with modest results.

More recent approaches introduced the concept of conditionally replicative adenoviruses CRAds where the transcriptional regulation of E1A expression, which drives viral replication, is under the control of a tumor specific promoters (TSPs). These CRAds provide a personalized approach because viral activity mostly occurs in cells expressing the gene from which the promoter has been selected.[15] Moreover, targeting specificity can be improved by pseudotyping the virus with non-native fibers obtained from other viral strains or by genetic modifications that can retarget the virus through non-natural receptors.[16,17] Although these modified

The first two authors contributed equally.

Correspondence: *Osvaldo L Podhajcer, Fundación Instituto Leloir, IIBBA-CONICET, Buenos Aires, Argentina. E-mail: opodhajcer@leloir.org.ar or Martín Montecino, Centro de Investigaciones Biomédicas and FONDAP Center for Genome Regulation, Universidad Andres Bello, Santiago, Chile. E-mail: mmontecino@unab.cl*

viruses are safe, improvement in therapeutic terms remained low due to restricted viral spreading in desmoplastic tumors, and the resistance of malignant cells to incorporate a sufficient amount of virus and the low expression levels of the gene regulated by the TSP.

Cancer development may result from global changes driven by the epigenetic machinery that includes DNA methylation, histone modification, and nucleosome positioning. In eukaryotic cells, DNA is packaged in arrays of particles called nucleosomes, which correspond to a 147 bp stretch of DNA wrapped around an octameric core of histones.[18] This structure, which contains ~1.7 turns of DNA, enforces DNA bending and regulates the binding of proteins that act as repressors or activators of gene expression to cognate DNA target sites.[18] Several reports indicate that modifications in DNA-histone interactions and the recruitment of chromatin remodeling complexes alter and displace nucleosomes, thereby modifying the structure of chromatin and allowing or inhibiting gene transcription.[19–22] We showed that a tissue regulatory element located within the proximal region of the osteocalcin gene promoter is a recognition site for the heterodimer CBFα/AML/PEBP2α.[20,21] A novel 182 bp nucleosome positioning sequence (NPS) in the osteocalcin promoter is responsible for positioning a nucleosome upstream of the CBFα binding site, leaving this element partially exposed and providing a spatial organization of the promoter that allows functional interactions between distally and proximally bound promoter elements.[20,21]

One of the strategies to boost the activity of promoters with invariably low transcriptional capacity is to add motifs responsive either to tumor microenvironmental conditions or to deregulated, constitutively active intracellular pathways. One of the paradigms for the latter in GICs is the Wnt/β-catenin signal transduction cascade.[23,24] Mutations in the genes encoding the Wnt signaling components APC, axin and β-catenin occurs in 30–70% of GICs, leading to the activation of Wnt-dependent target genes.[23–25] Only a few reports have studied the effect of TCF/LEF responsive sequences as heterologous enhancers to augment the transcriptional activity of a given promoter.[26–29] We have previously characterized the promoter region of the *COX-2* gene and identified a 0.8 kb Wnt/β-catenin responsive region demonstrating high transcriptional activity.[30] This region contains a novel TCF/LEF response element (TBE site-II) that directly responds to Wnt/β-catenin signaling. We hypothesized that a chimeric enhancer

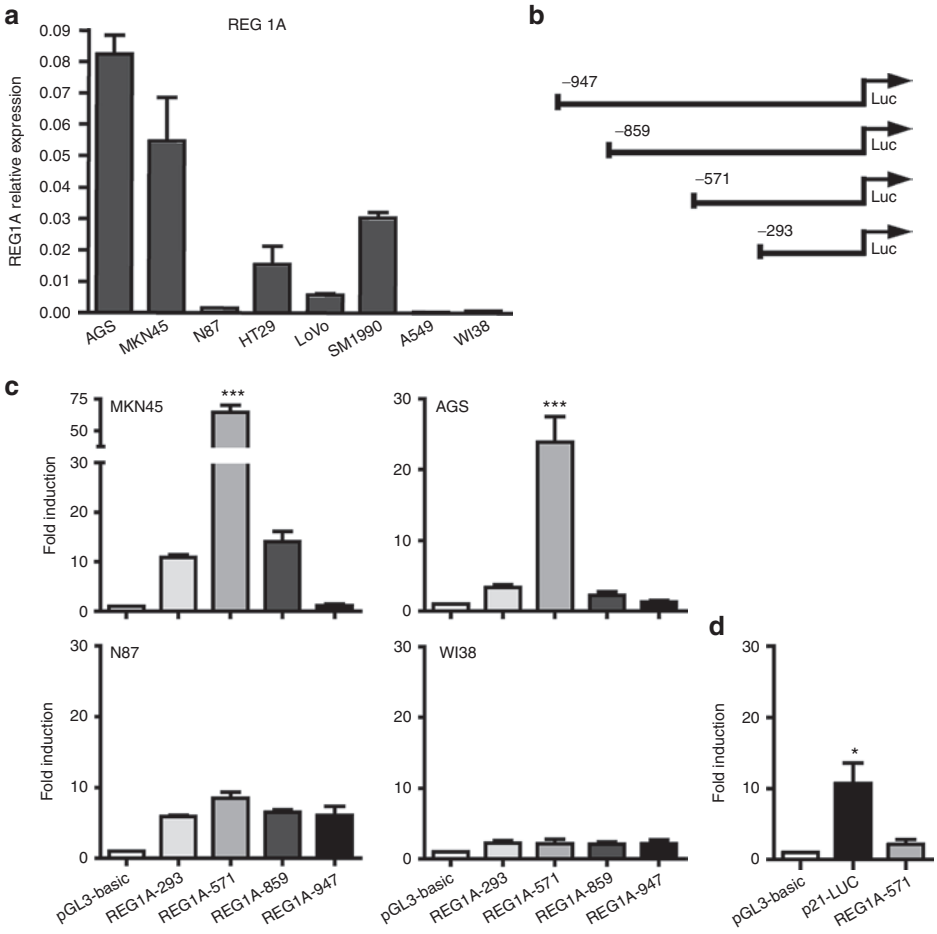

Figure 1 REG1A promoter activity. (**a**) Quantitative determination of REG1A mRNA expression by qPCR. β-actin was used as an internal control. (**b**) Schematic representation of REG1A promoter variants. (**c**,**d**) Cells were transiently transfected with 100 ng of the different constructs and assessed for luciferase activity. Cells were cotransfected with 1 ng of PRL-SV40 Renilla as an internal control. Promoter activity was normalized as the ratio between firefly luciferase and Renilla and expressed as the fold induction over empty vector. Each figure represents at least three independent experiments. Statistical significance was determined using analysis of variance (*$P < 0.05$; ***$P < 0.001$).

sequence comprising Wnt-responsive elements combined with the NPS of the osteocalcin promoter might improve the transcriptional activity of GIC-specific promoters. Here, we demonstrate that a chimeric sequence named pART, which is composed of four tandemly repeated COX-2 TBE site-II elements cloned upstream of the osteocalcin NPS signal, enhanced the activity of the human *REG1A* gene promoter, driving the replication and lytic capacity of a conditionally replicative adenoviruses (CRAd). Importantly, the *in vitro* and *in vivo* activity of the CRAd was strictly dependent of the presence of the NPS because deletion of this sequence abolished the enhancer effect of pART. Moreover, the NPS also enhanced the responsiveness of additional responsive elements.

RESULTS

Design and assessment of the enhancer activity of the hybrid artificial enhancer pART

To take advantage of the specific structural features of the nucleosomes placed between regulatory elements,[20] we designed the chimeric enhancer pART by placing four tandemly repeated copies of the TCF/LEF-responsive element (TBE) from the human *COX-2* gene promoter (−692 bp to −683 bp)[30] upstream of the NPS from the rat osteocalcin gene promoter (−286 bp to −106 bp).[21] The transcriptional capacity of pART was initially assessed by cloning downstream a specific fragment from the human *REG1A* gene, which has been described to be differentially expressed in gastric, pancreatic and colon cancer compared with adjacent non-malignant tissue.[31–33]

REG1A mRNA was expressed at high levels in AGS and MKN45 gastric cancer cell lines and SW1990 pancreatic cancer cells; HT29 and Lovo colorectal cancer cells expressed moderate levels of REG1A mRNA, whereas N87 gastric cancer cells did not exhibit significant expression of this gene (**Figure 1a** and **Supplementary Figure S1**). WI38 human fetal lung fibroblasts and A549 human lung carcinoma cells that were used as non-GIC control cells did not express detectable levels of REG1A (**Figure 1a** and **Supplementary Figure S1**).

We next cloned a 1.0 kb fragment of the human *REG1A* gene promoter (extending from −947 bp to +75 bp) that includes, among other elements, a non-functional TBE motif (data not shown) and a TATA box sequence (**Supplementary Figure S1b**). The 1.0 kb REG1A promoter fragment (pREG1A-947) and shorter versions of this fragment (**Figure 1b**) were placed upstream of the luciferase reporter gene. The 1.0 kb fragment was unable to drive significant luciferase activity when transiently transfected into the REG1A mRNA-positive MKN45 and AGS gastric cancer cells (**Figure 1c**). However, the deletion of 0.1 kb from the 5′-end (pREG1A-859-Luc) and the deletion of 0.4 kb from the 5′-end (pREG1A-571-Luc) in particular induced strong REG1A promoter activity in MKN45 and AGS gastric cancer cells compared with the other promoter fragments (**Figure 1c**). A further 0.7 kb deletion (pREG1A-293-Luc) resulted in a significant reduction in the promoter activity (**Figure 1c**), suggesting that the −571/−293 fragment contains the key regulatory elements that activate *REG1A* gene transcription. REG1A promoter activity was extremely low in N87 gastric cancer cells, which is consistent with the low levels of REG1A mRNA expression in this cell line (**Figure 1c**). As expected, none of the promoter fragments showed any activity in REG1A-negative WI38 fibroblasts. The lack of REG1A promoter activity in WI38 cells was not due to reduced transfection efficiency because other transiently transfected promoter-reporter constructs, such as the p21 gene promoter, exhibited high levels of transcriptional activity (**Figure 1d**), confirming that REG1A promoter activity specifically occurs in cells expressing REG1A mRNA.

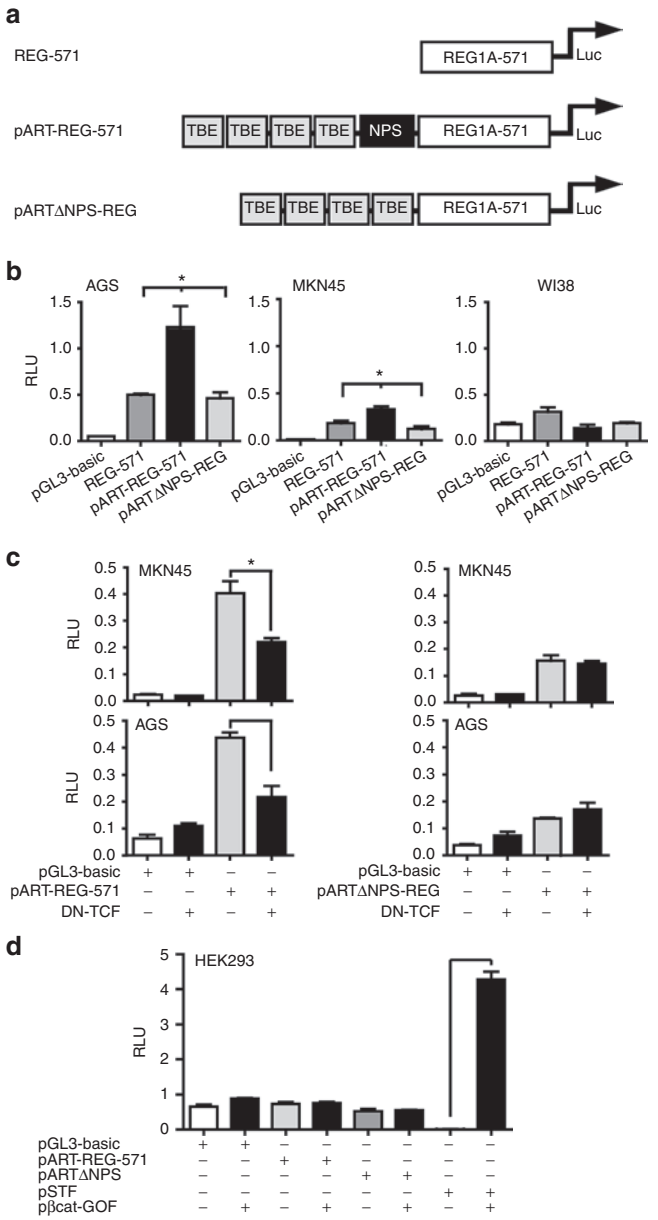

Figure 2 Enhancement of the REG1A promoter activity by the NPS and Wnt-responsive elements. (**a**) Schematic representation of the different constructs. (**b**) Gene reporter assays to assess the role of the NPS. Cells were transiently transfected with different constructs with or without pART and the NPS and assessed for luciferase activity. (**c**) Cells were transiently transfected with the different constructs and cotransfected with or without a dominant-negative mutant (DN-TCF) of the TCF/LEF transcription factor. (**d**) Gene reporter assays in HEK-293 cells transfected with the different constructs in the presence or absence of a construct expressing β-catenin. SuperTOPFLASH (STF) promoter was used as a control for β-catenin activity. Each figure represents at least three independent experiments (*$P < 0.05$).

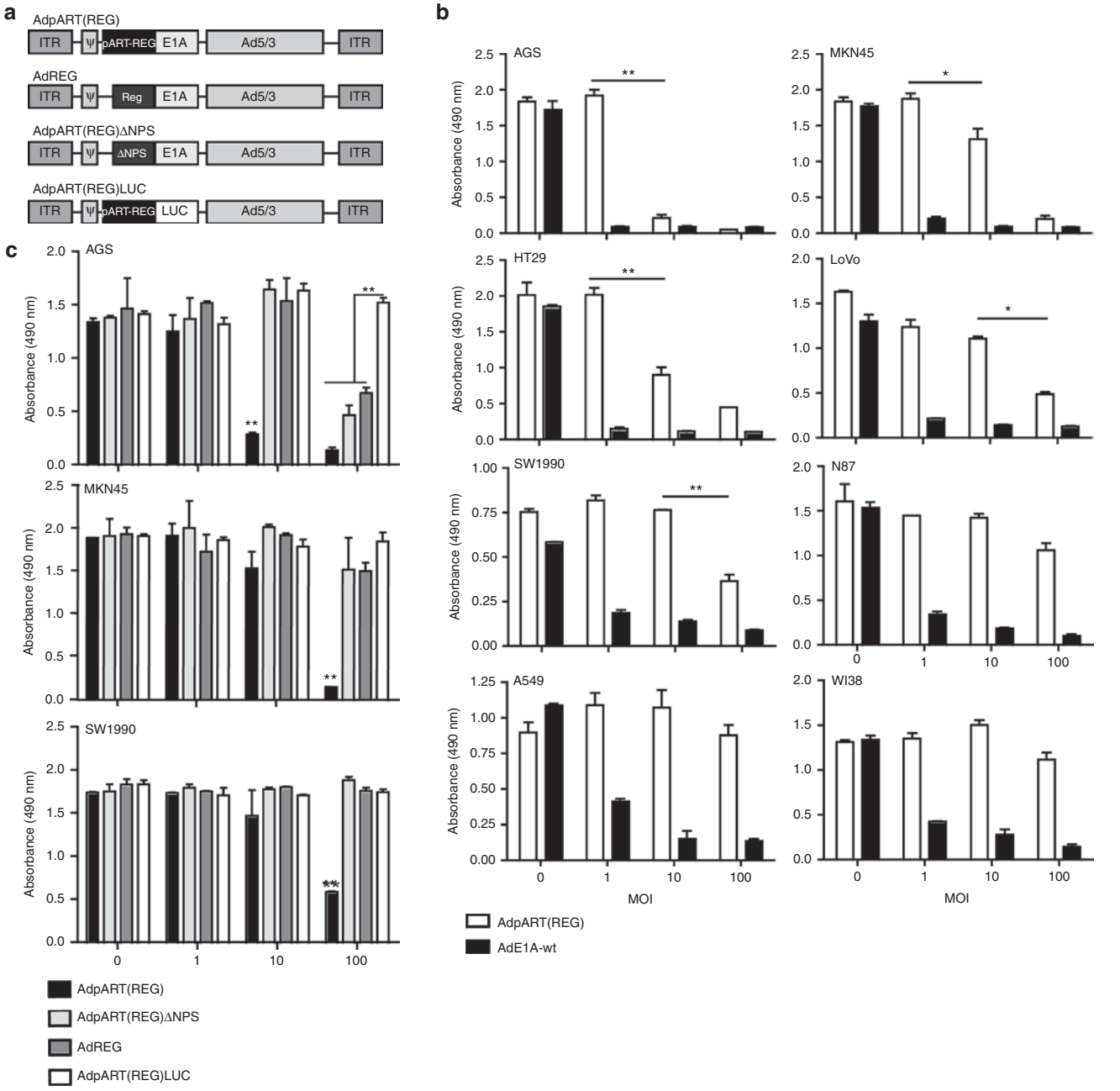

Figure 3 *In vitro* **lytic activity of the CRAd carrying pART.** (**a**) Schematic representation of the CRAds constructs. (**b**) Cells were exposed to different multiplicity of infections for 6 days followed by the assessment of cell viability with 3-(4,5-dimethylthiazol-2-yl)-5-(3-carboxymethoxyphenyl)-2-(4-sulfophenyl)-2H-tetrazolium (MTS). (**c**) Similar to the previous panel. Each figure represents at least three independent experiments. Statistical significance was determined using analysis of variance test (*$P < 0.05$, **$P < 0.01$).

On the basis of the previous data, we decided to place REG1A-571 downstream of the pART synthetic enhancer to generate pART-REG (**Figure 2a**). The transient transfection of pART-REG in MKN45 and AGS gastric cancer cells led to significantly higher (~2-fold) luciferase activity compared with REG-571 (**Figure 2b**). This enhanced promoter activity was strictly dependent on the NPS because pARTΔNPS, which lacks the NPS, exhibited transcriptional activity equivalent to that shown by REG-571 (**Figure 2b**). Importantly, pART had no effect on the transcriptional activity of REG1A in REG1A-negative WI38 fibroblasts and human embryonic kidney HEK-293 cells (**Figure 2d**), indicating that pART-enhanced REG1A activity exclusively in cells where the promoter is already active. Moreover, the NPS showed no enhancer activity itself (data not shown).

We next determined whether the Wnt/β-catenin responsiveness contributes to the enhanced activity exerted by pART. pART-REG activity was reduced by almost 50% upon coexpression of the dominant-negative mutant DN-TCF, indicating that the Wnt/β-catenin responsive elements participate in the enhancement of the REG1A activity induced by pART (**Figure 2c**). As a control,

we observed that enforced expression of DN-TCF also inhibited SuperTOPFLASH reporter activity (**Supplementary Figure S2**). Notably, DN-TCF did not affect pARTΔNPS-REG activity (**Figure 2c**), indicating that the TBE sites contribute to pART-REG-571 activity only when the NPS sequence is present (**Figure 2d**). Taken together, these results indicate that the transcriptional activity of pART-REG requires the presence of the NPS, which facilitate a functional interaction between the REG-571 promoter and the distal tandem repeat in Wnt/β-catenin responsive elements.

pART enhances the lytic capacity of an oncolytic adenovirus

We next evaluated the ability of pART-REG to drive the lytic activity of a CRAd pseudotyped with a 5/3 fiber. For this purpose, we cloned pART-REG in front of the early adenoviral gene *E1A* to obtain AdpART(REG) (**Figure 3a**). To further confirm the contribution of pART and the NPS to the lytic activity of AdpART(REG), we constructed an AdREG that lacks pART and an AdpART(REG)ΔNPS that lacks the NPS and the non-replicative virus AdpART(REG)LUC (**Figure 3a**). The *in vitro* lytic capacity of AdpART(REG) was evaluated in REG1A mRNA-positive cells (AGS, MKN45, SW1990, HT29, and LoVo) and REG1A mRNA-negative A549 lung cancer cells and WI38 fibroblasts. AdpART(REG) exhibited the highest lytic activity on AGS gastric cancer cells (at 10 multiplicity of infection), which is consistent with the highest REG1A mRNA levels expressed by this cell line (**Figure 3b**). Significant lytic activity was also observed on MKN45 gastric and HT29 colon cancer cells, whereas LoVo colon and SW1990 pancreatic cancer cells were more resistant to the CRAd lytic activity (**Figure 3b**), which is likely due in part to the less efficient infectivity of these cells by the 5/3 pseudotyped virus (**Supplementary Figure S3**). As expected, an almost complete absence of lytic activity for AdpART(REG) was observed on REG1A mRNA-negative N87, A549 and WI38 cells (**Figure 3b**). Thus, AdpART(REG) showed attenuated but highly specific activity compared with AdE1A-wt (**Figure 3b**). In agreement with the results using transiently transfected constructs, the cytopathic activity of AdpART(REG) was strongly dependent on the presence of the NPS. Indeed, removal of the NPS led to a great reduction in the lytic activity of AdpART(REG) on gastric and pancreatic cancer cells (**Figure 3c**).

To establish whether the pART effect is associated with the enhancement of viral E1A expression levels, we transduced REG1A-positive cells with AdpART(REG) and AdREG. Cell extracts were obtained at different time points post-infection to evaluate E1A expression by quantitative real-time PCR (qRT-PCR) and western blot. E1A mRNA expression was detectable 2 hours after infection with AdpART(REG) (**Figure 4a**,**b**) but only 8–24 hours after infection with AdREG (**Figure 4a**,**b**). Consistent with this result, the E1A protein was detected only after 8 hours, following infection with AdpART(REG), whereas it was almost undetectable after infection with AdREG (**Figure 4c**). As a control, we observed no E1A mRNA expression following the infection of REG1A-negative A549 lung cancer cells with AdpART(REG), whereas the wild type virus induced E1A mRNA expression immediately after 2 hours (**Supplementary Figure S4**). Taken together, these data suggest that pART is a potent enhancer of the transcriptional activity of the REG1A promoter, increasing the lytic activity of AdpART(REG) by stimulating E1A transcription and hence viral replication.

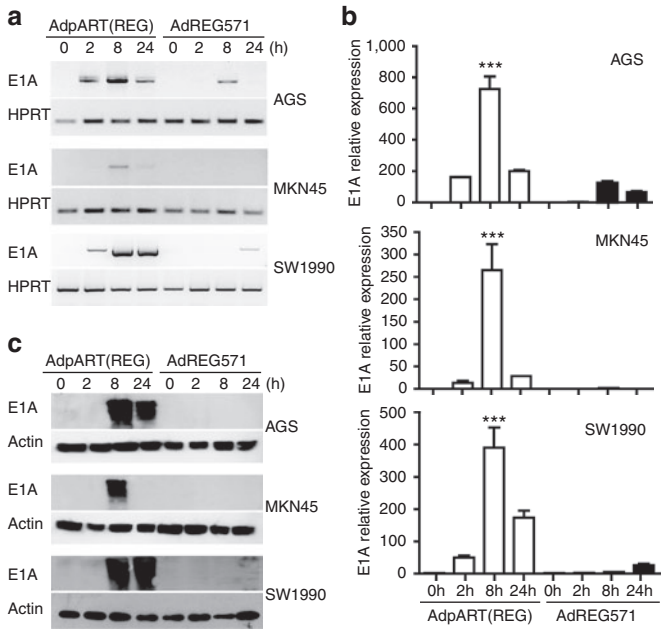

Figure 4 Enhancement of E1A expression by pART. (**a**) E1A mRNA expression in cells exposed to 100 multiplicity of infection (MOI) of the different viruses. HPRT mRNA levels were used as an internal control. (**b**) Quantification of the data in **a** in arbitrary units of E1A relative to the HPRT levels. (**c**) Western analysis of E1A expression using β-actin (actin) as an internal control. Each figure represents at least three independent experiments. Statistical significance was determined using analysis of variance (***$P < 0.001$).

In vivo analysis of the therapeutic potential of the CRAd carrying pART

Once the *in vitro* lytic capacity of AdpART(REG) was confirmed, we proceeded to study its *in vivo* therapeutic efficacy. In preliminary studies, we xenografted SW1990 pancreatic cancer cells s.c. in male nude mice. When tumors reached an average size of 100 mm^3, the mice were administered three doses of either 1×10^8 viral particles of AdpART(REG) or vehicle. The administration of AdpART(REG) significantly reduced the *in vivo* growth of SW1990 tumors in 4/5 animals (**Figure 5a**). In only one case, a mouse that received AdpART(REG) developed a tumor at a size comparable with that observed in the control group (**Figure 5a**).

To further confirm the therapeutic efficacy of AdpART(REG) and the role of the NPS, we orthotopically xenografted SW1990-mcherry-LUC cells in mouse pancreases. Mice harboring 10-day-old established tumors were split in four groups and administered i.p. with one dose of 1×10^9 vp of AdpART(REG), AdpART(REG)ΔNPS, AdREG, or AdpART(REG)LUC. Mice were followed in real time with a bioluminometer and killed 30 days after viral administration. Following assessment at necropsy (**Figure 5b**), we observed that only the group of mice treated with AdpART(REG) showed a statistically significant reduction in tumor volume and weight compared with the control mice (**Figure 5c**). Tumors in mice injected with AdREG or AdpART(REG)ΔNPS showed no significant

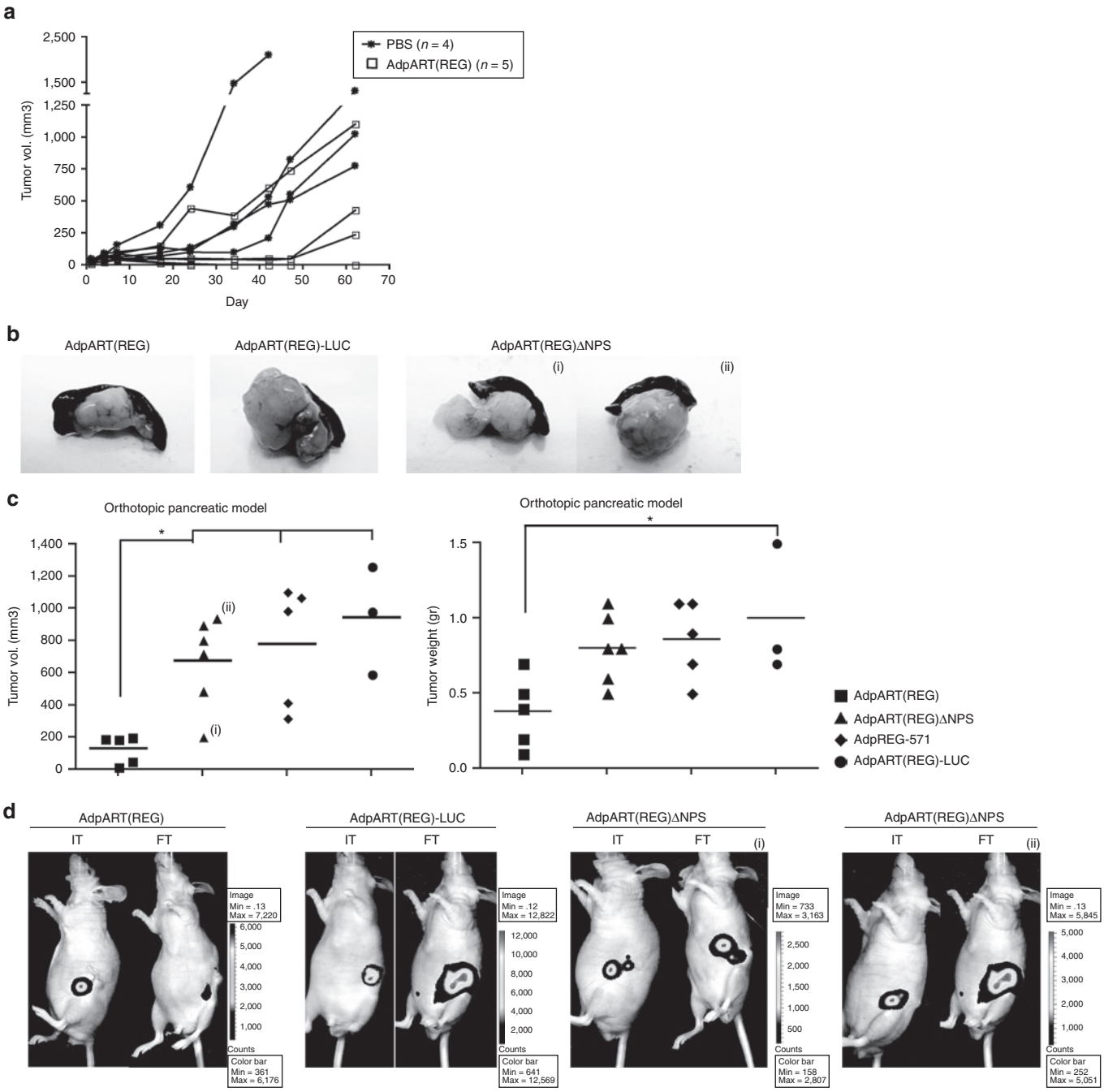

Figure 5 AdpART-REG-E1A effect on the *in vivo* growth of human pancreatic cancer xenografts. (**a**) S.c. growth of SW1990 cells in nude mice treated with AdpART(REG) or vehicle. Each line represents a single mouse. The arrows indicate the time of viral (or vehicle) administration. (**b**) Representative macroscopic images of orthotopic pancreatic tumors 30 days after viral administration. (**c**) The tumor volumes and weights corresponding to mice treated with the different viruses. All measurements were obtained with double blind measurement. Statistical significance was determined using analysis of variance (*$P < 0.05$). (**d**) Representative whole-body images of bioluminescence activity of mice harboring SW1990 m-cherry-Luc tumors. Images were obtained on days 1 and 30 after viral administration. FT, final time; IT, initial time.

difference compared with the control (Figure 5c), demonstrating that either the absence of pART or the deletion of the NPS strongly reduced the antitumor efficacy of the CRAd. Although AdpART(REG)ΔNPS and AdREG were unable to significantly inhibit tumor growth as a whole, we observed a clear antitumor effect in one to two mice (see Figure 5c and the comparison of the two mice treated with AdpART(REG)ΔNPS in Figure 5d), suggesting that these CRAds might exhibit a partial antitumor activity that is enhanced when the virus included pART.

pART enhances the transcriptional activity of additional TSPs

To establish whether pART can enhance the transcriptional activity of additional heterologous promoters, we prepared a

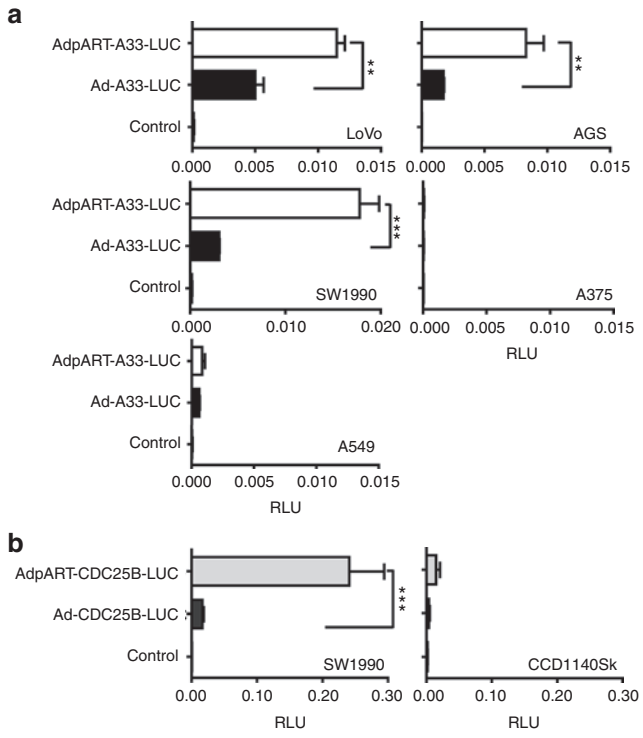

Figure 6 pART enhancement of the transcriptional activity of additional promoters. Transcriptional activity of non-replicative adenoviruses expressing luciferase under the control of the (**a**) A33 or (**b**) cdc25b promoters. Cell extracts were assayed 48 hours afterward for firefly and Renilla luciferase. Data are shown as relative luciferase units (RLU) normalized to Renilla. Each column represents the mean ± SD ($n = 3$). Statistical significance was determined using the analysis of variance test (**$P < 0.01$, ***$P < 0.001$).

non-replicative adenovirus by subcloning pART upstream of the human colon cancer-specific A33 TSP to drive luciferase expression.[34] We observed more than a two-, four-, and eightfold increase in the transcriptional activity of pART-A33 in REG1A-positive LoVo, AGS, and SW1990 malignant cells, respectively, compared with the A33 promoter alone (**Figure 6a**). No pART enhancement was observed in the REG1A-negative A549 lung cancer and A375 melanoma cells (**Figure 6a**). Consistent with the results obtained with the REG1A and A33 promoter, pART also induced a 10-fold increase in the transcriptional activity of a 0.4 kb cdc25b gene promoter sequence (Weber *et al.*, manuscript submitted) in cdc25b-positive SW1990 pancreatic cancer cells (**Figure 6b**). A slight, but non-statistically significant increase was also observed in the cdc25b-negative skin fibroblasts CCD1140Sk (**Figure 6b**). pART enhancement was consistent with the nuclear levels of β-catenin in the different cell lines because the largest enhancement was observed in SW1990 cells that exhibited the highest β-catenin expression levels (**Supplementary Figure S5**).

NPS enhanced the responsiveness of hypoxia- and NFκB-responsive elements

To further establish the capacity of the NPS to enhance the activity of additional responsive sequences, we replaced the Wnt-β-catenin responsive elements in pART with hypoxia (HRE)- and NFκB (NF-RE)-responsive elements[35] upstream of the REG1A promoter to drive luciferase expression. The transient transfection of REG1A-positive AGS and LoVo malignant cells with the expression constructs showed a dramatic enhancement in the activity of the chimeric promoters containing either an HRE or NF-RE (**Figure 7**). Moreover, HRE activation occurred only under hypoxia but not under normoxia (**Supplementary Figure S6**). HRE and NF-RE enhancement was strictly dependent on the NPS because its removal from the constructs abrogated the enhanced transcriptional activity (**Figure 7**). In addition, the constructs containing the NPS and the responsive elements were unable to induce a significant change in the REG1A promoter activity in A549 and A375 cells lacking REG1A expression (**Figure 7**), stressing the high stringency of the synthetic enhancers.

DISCUSSION

DNA promoter regions determine the initiation rates of transcription by acting as anchoring platforms for the RNA polymerase II complex.[36] These sequences interact with cell specific transcriptional microenvironments, altering the chromatin structure and hence regulating gene expression.[37] On the basis of these well-established general concepts of transcriptional regulation, we designed an artificial chimeric enhancer, pART, which contains four Wnt-responsive elements positioned upstream of a NPS. pART proved to be effective in increasing the transcriptional activity of the REG1A promoter without altering its specificity, and it efficiently enhanced the replication and therapeutic efficacy of an oncolytic adenovirus.

To validate the enhancer capacity of pART, we selected the REG1A gene promoter as a novel TSP. REG1A mRNA is highly upregulated in GIC.[31–33] We showed that a promoter fragment that spans 571 bp is necessary and sufficient to function as a TSP and drives the replication of an oncolytic adenovirus. Despite our previous study of the human *COX-2* gene in GIC cells,[30] we avoided using the *COX-2* gene promoter instead of REG1A because COX-2 is highly expressed during tissue inflammatory processes, raising the potential risk of increasing collateral unwanted effects *in vivo*.[38] The recombinant pART/REG1A promoter was active in an adenoviral context in different GIC cell lines such as the gastric cancer cells MKN45 and AGS, the pancreatic cancer cells SW1990 and the colon cancer cells LoVo and HT29; the lack of activity in WI38 fibroblasts and A549 lung cancer cells indicates that pART/REG1A can be widely useful in a wide variety of types of GICs. Most importantly, AdpART(REG) was also able to strongly inhibit the *in vivo* growth of orthotopic pancreatic tumors following the direct intra-tumor administration of the CRAd. Our *in vitro* data confirmed that pART-enhanced E1A transcriptional expression, which is reflected by its detection as early as 2 hours after infection. CRAds lacking pART only produced detectable E1A expression 8 hours after infection. Although the REG1A promoter attenuated viral lytic activity compared with the wild type virus, it maintained a high specificity when driving viral replication alone or when pART was included in the construct; indeed, the resulting CRAd was active only in REG1A-positive cells, whereas the wild type virus was highly lytic regardless of REG1A expression.

Different regulatory sequence motifs have been used in the past to increase the transcriptional activity of TSPs and enhance the potency of oncolytic viruses. Generally, these types of studies

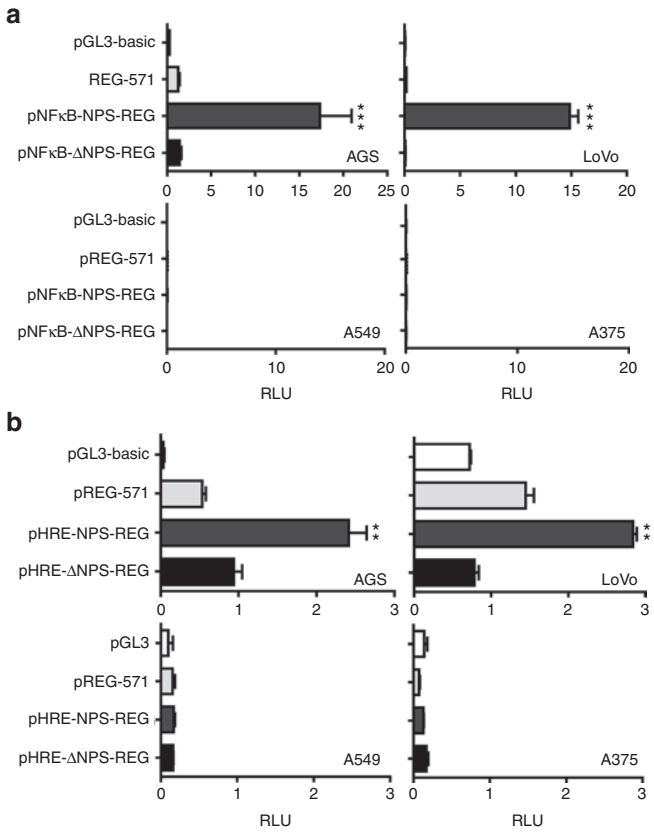

Figure 7 Enhancer activity of hypoxia- and NFκB-responsive elements placed upstream of the NPS. (**a**) Gene reporter assays with different constructs containing NFκB- or HRE-responsive elements and NPS. (**b**) Cells were transiently transfected with different constructs and assayed for luciferase activity under normoxic or hypoxic (1% O_2) conditions. Data are shown as relative luciferase units (RLU) normalized to Renilla. Each column represents the mean ± SD (n = 3). Statistical significance was determined using analysis of variance (**P < 0.01, ***P < 0.001).

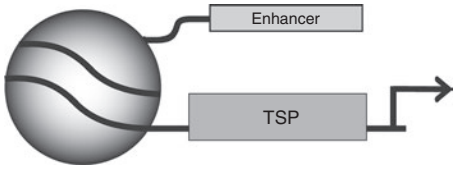

Figure 8 Schematic representation of the potential spatial conformation of Enhancer-NPS-TSP sequences in the nuclear environment.

focused on motifs responsive to the tumor microenvironment including hypoxia, inflammation and reactive oxygen species.[39,40] Elements that respond to tissue-specific and constitutively active signaling pathways include those responsive to the Wnt/β-catenin pathway in GIC cells[26–29] and estrogen or androgen responsive motifs in breast or prostate cancer, respectively.[41,42] Here, we have used for the first time a sequence that positions nucleosomes, a chromosomal structure that can define spatial features and the functional organization of the transcriptional machinery at gene promoters. The enhanced activity exerted by pART was highly dependent on the presence of the NPS because deletion of this region completely obliterated not only the pART enhancer effect but also the *in vitro* and *in vivo* efficacy of the CRAds. It was unexpected that the removal of the 200 bp NPS from pART, which brings the Wnt-responsive motifs closer to the transcription initiation site, would result in the loss of enhancement activity. Thus, we suggest that the role of the NPS is to bring the Wnt-responsive elements in close spatial proximity to the REG1A promoter regulatory elements to enhance promoter activity (**Figure 8**). A special juxtaposition that brings proximal and distal Wnt-responsive sites close to the transcription start site has been recently described.[43]

Both the *in vitro* and *in vivo* studies confirmed the strict dependence of viral activity on the presence of the NPS. Interestingly, pART was also able to enhance the transcriptional activity of other TSPs in an adenoviral context. In addition, pART was also able to increase the transcriptional activity of the non-tumor-related, neural enolase promoter (**Supplementary Figure S7**). Finally, the presence of the NPS was a *sine qua non* condition for the responsiveness of not only the Wnt-β-catenin-responsive element but also the hypoxia- and NFκB-responsive elements. Indeed, removal of the NPS completely abrogated the enhanced transcriptional activity induced by the three different responsive elements. The incorporation of pART led to significantly improved TSP and CRAd activity *in vitro* and *in vivo*. On the basis of all of the data present in this study, it can be concluded that the use of NPSs could be a useful tool for gene therapy approaches in cancer and other human diseases as well.

MATERIALS AND METHODS

Cell lines. The human pancreatic cancer cells SW1990, colorectal cancer cells LoVo and HT29, gastric cancer cells AGS and N87, lung carcinoma cells A549, melanoma cells A375, fetal lung fibroblasts WI38, skin fibroblasts CCD1140Sk cells, and human embryonic kidney cells (HEK-293) were obtained from the ATCC (American Tissue Culture Collection, Rockville, MD). The gastric cancer cells MKN45 (Japanese Collection of Research Bioresources, Japan) were generously donated by Andrew Quest (University of Chile). All of the cell lines were grown following the manufacturer's recommendations for culture media, supplements and antibiotics in a 37 °C atmosphere containing 5% CO_2.

Plasmid vectors. SuperTOPFlash-luciferase, the pRL-SV40 plasmid,[30] the constitutive active β-catenin (S33Y) β-cat-GOF,[44] and the dominant-negative pDN-TCF4 expression plasmids[25] have been previously described. The REG1A-947 promoter was obtained by high fidelity PCR amplification from human genomic DNA using the following primers: pREG1A-947-Fwd and pREG1A-Rev (**Supplementary Table S1**). This DNA fragment (positions −947 to +75) was cloned into the pGL3-basic plasmid (Promega, Madison, WI). REG1A-859, and REG1A-293 were generated by PCR with the pREG1A-859-Fwd, pREG1A-293-Fwd, and pREG1A-Rev primers (**Supplementary Table S1**) using the pGL3-REG1A-947 plasmid as a template. The REG1A-571 plasmid was obtained from pGL3-REG1A-947 by cleaving with the *Hind*III and *Bgl*II restriction enzymes (New England Biolabs, Ipswich, MA). For pART plasmid construction, an oligonucleotide containing a multimerized copy (4X) of the TCF/LEF responsive element (TBE) from the COX-2 promoter (site-II)[30] was obtained by chemical synthesis, and it was introduced into pART with the *Kpn*I and *Xho*I restriction sites (New England Biolabs, Ipswich, MA). The NPS was obtained from the rat osteocalcin promoter using high fidelity PCR amplification with the NPS-Fwd and NPS-Rev specific primers (**Supplementary Table S1**), which contain *Xho*I and *Sac*I restriction sites. The resulting 182 bp fragment was linked to the 4XTBE sequence after cleavage at the *Xho*I site (New England Biolabs, Ipswich, MA) and ligated using T4 ligase (New England Biolabs, Beverly, MA). Finally, this cassette (4XTBE-NPS) was linked to the REG-571 promoter sequence by Sac*I* restriction site

cleavage/ligation (resulting in the 4XTBE-NUC-REG571 sequence) and inserted in the pGL3-basic vector in the *Kpn*I and *Bgl*II restriction sites (New England Biolabs, Ipswich, MA). The pARTΔNPS plasmid was generated by cleavage with the *XhoI* and *SacI* restriction enzymes (New England Biolabs, Ipswich, MA). The pGL3-NSE promoter was obtained from Addgene (plasmid 11606) (Addgene, Cambridge, MA). pGL3-pART-NSE was constructed by the insertion of pART into the pGL3-NSE plasmid in the *Nhe*I/*Bgl*II restriction sites. The pNFκB-NPS-REG and HRE-NPS-REG constructs were generated from pART-REG-571 by 4xTBE sequence cleavage (*Kpn*I/*XhoI*)and insertion of the NFκB and HRE enhancers[35] into the *Kpn*I/*SmaI* and *Kpn*I/*StuI(Klenow)* restriction sites, respectively. Successful cloning was confirmed by restriction enzyme digestion analyses and automated sequencing.

Adenoviral construction. The pART-REG-571, pART-ΔNPS, and REG-571 promoters were cloned upstream of the E1A or Luciferase (LUC) genes into adenoviruses containing the chimeric fiber 5/3.[45] The pART-REG-571 promoter was isolated from the pGL3-pART-571 construct by digestion with the *Kpn*I/*Bgl*II restriction enzymes (New England Biolabs, Ipswich, MA) and subcloning into the pShuttle-1 vector (Stratagene, La Jolla, CA) followed by E1A or LUC[45] in the *Xba*I/*Sal*I sites, hence producing pShuttle-pART(REG)-E1A or pShuttle-pART(REG)-LUC (also pShuttle-REG-E1A and pShuttle-ΔNPS-E1A). AdpART-A33-LUC and AdpART-CDC25B-LUC were generated by the subcloning of pART upstream of the A33[34] or cdc25B (Weber *et al*., manuscript submitted) gene promoters following the methodology described above, resulting in the pShuttle-pART-A33-LUC and pShuttle-CDC25B-LUC constructs, respectively. Viral constructs containing the chimeric promoters were prepared using previously available backbones and shuttle vectors followed by viral stock production.[45]

Luciferase reporter assays. Cell lines grown in 24-well plates were transfected using FUGENE 6 (Roche Applied Science, IN) following the manufacturer's indications. Different amounts of the described plasmids were assayed for 24 hours. The cells were then collected and assayed for Firefly and Renilla Luciferase activities (Promega) using a Genius luminometer (TECAN, Maennedorf, Switzerland). Each of these experiments was performed at least three times. For assays using adenoviruses, luciferase assays followed Lopez *et al*.[44] The luciferase activity was normalized by the total protein concentration in the cell lysate.

In vitro *cytotoxicity assay.* To determine the virus-mediated cytotoxicity, 1×10^4 cells were seeded in 24-well tissue culture plates and infected with CRAds at the indicated multiplicity of infections. After 6 days, cell viability was measured as described.[44]

mRNA expression. RNA extraction and RT-PCR assays were performed as previously reported.[30] The mRNA was measured by qRT-PCR in an Mx 3005p qPCR thermocycler (Stratagene) using specific primers (**Supplementary Table S1**). PCR conditions were as follows: an initial denaturation for 150 seconds at 94 °C followed by 39 cycles of 45 seconds at 94 °C, 30 seconds at 60 °C and 30 seconds at 72 °C. All reactions were performed in triplicate. In this assay, HTRP gene expression was measured as an internal control using the HTRP-Fwd and HTRP-rev specific primers (**Supplementary Table S1**).

Assessment of E1A levels. To determine the E1A mRNA levels, 1.5×10^6 cells per well were seeded in a six-well plate. The next day, the cells were infected with the indicated viruses at a 500 multiplicity of infection. After 2, 4, 8, and 24 hours, cells were lysed, and total RNA was obtained. A quantitative and semi-quantitative PCR for E1A RNA was performed using specific primers (Q-E1A-Fwd and Q-E1A-Rev and F-E1A-560-Fwd and R-E1A-1632 Rev; See **Supplementary Table S1**). For western blot studies, cells were transduced with the different viruses at 500 multiplicity of infection. Total protein extraction and western blots were performed as described.[45] The membrane was probed with an anti-E1A antibody (M73; Santa Cruz Biotechnology, Santa Cruz, CA), and an anti-β-actin antibody (A4700; Sigma, St Louis, MO) was used as a loading control. To analyze the β-catenin protein in the GIC cell lines, nuclear extracts were prepared as previously reported.[46] Protein levels were quantified by the Bradford assay using bovine serum albumin as a standard. Primary antibodies used included β- catenin (sc-1496; Santa Cruz Biotechnology) and anti-Histone H3, pan, clone A3S (05-928, Millipore, Billerica MA) as an internal control.

In vivo *studies.* Five- to six-week-old female and male athymic N:NIH (S)-nude mice (obtained from the animal facility of the Faculty of Veterinary, Universidad de La Plata, Argentina) were s.c. injected in one flank with 5×10^6 SW1990 cells. Tumor volumes were estimated once a week from caliper measurements using the following formula: volume = $0.52 \times (\text{width})^2 \times \text{length}$. For orthotopic studies, mice were anesthetized via the i.p. injection of 80 mg/kg ketamine (Aveco, Fort Dodge, IA) and 10 mg/kg xylazine (Rugby Laboratories, Rockville, MD). A small (1 cm) lateral subcostal laparotomy was performed. A total of 5×10^5 SW1990 cells suspended in 50 ml phosphate-buffered saline were injected beneath the capsule of the pancreas. Following cell injection, cell bleeding or leakage from the pancreas was stopped by applying Matrigel (Matrigel Basement Membrane Matrix, BD Biosciences, Franklin Lakes, NJ) to the site of injection, and the abdominal wall and skin were closed. At the end of the experiments (40 days post adenoviral injection), the mice were euthanized. Twice weekly, whole-body images of each mouse were obtained with a bioluminescence assay. Animals were anesthetized, and the D-Firefly-Luciferin substrate (Xenogen, Alameda, CA) was administered intraperitoneally (32 mg/kg). Luciferase activity was visualized using an *in vivo* bioluminescence system (IVIS50; Xenogen) and Living Image 2.20.1 Software. *In vivo* experiments were performed following the institutional guidelines approved by the NIH (see below), and all animals under study received food and water *ad-libitum*. *In vivo* experiments were approved by the Institutional Animal Care and Use Committee of Instituto Leloir.

Statistical analysis. Each *in vitro* experiment was repeated at least three times with three replicates. Data are shown as the means ± SD. Multiple group comparisons were performed with one-way analysis of variance using the STATISTICA 9.0 software (Statsoft Inc., Tulsa, OK). A $P < 0.05$ was considered significant.

SUPPLEMENTARY MATERIAL

Figure S1. REG1A mRNA expression.
Figure S2. Wnt/β-catenin pathway control activity.
Figure S3. Levels of infectivity of an adenovirus pseudotyped with the chimeric fiber 5/3.
Figure S4. E1A mRNA expression assay.
Figure S5. Nuclear levels of the β-catenin protein.
Figure S6. Activity of the hypoxia responsive elements during normoxia.
Figure S7. Effect of pART on the enolase (NSE) promoter activity.
Table S1. Sequences of the primers used in this study.

ACKNOWLEDGMENTS

This study was supported by grants from the Programa Bicentenario—BancoMundial, Conicyt, Chile CTE-06 (to O.L.P. and M.M.) and FONDAP 15090007 (to M.M.). We are indebted to the continuous support of Amigos de la Fundación Instituto Leloir para la Investigación en Cancer (AFULIC) Foundation, Argentina. F.N. was supported by a postdoctoral fellowship from CONICET and the Organización de Estados Americanos. The authors declare no conflict of interest.

REFERENCES

1. Sutter, AP and Fechner, H (2006). Gene therapy for gastric cancer: is it promising? *World J Gastroenterol* **12**: 380–387.
2. Cathcart, M, O'Byrne, K, Reynolds, J, Sullivan, J and Pidgeon, G (2012). COX-derived prostanoid pathways in gastrointestinal cancer development and progression: Novel targets for prevention and intervention. *Biochim Biophys Acta* **1825**: 49–63.

3. Yang, X, Takano, Y and Zheng, HC (2012). The pathobiological features of gastrointestinal cancers (Review). *Oncol Lett* **3**: 961–969.
4. Herszényi, L and Tulassay, Z (2010). Epidemiology of gastrointestinal and liver tumors. *Eur Rev Med Pharmacol Sci* **14**: 249–258.
5. Bhattacharyya, M and Lemoine, NR (2006). Gene therapy developments for pancreatic cancer. *Best Pract Res Clin Gastroenterol* **20**: 285–298.
6. Watanabe, M, Baba, H, Ishioka, C, Nishimura, Y and Muto, M (2012). Recent advances in diagnosis and treatment for malignancies of the gastrointestinal tract. *Digestion* **85**: 95–98.
7. Jørgensen, JT and Hersom, M (2012). HER2 as a Prognostic Marker in Gastric Cancer - A Systematic Analysis of Data from the Literature. *J Cancer* **3**: 137–144.
8. Yamamoto, M (2004). Conditionally replicative adenovirus for gastrointestinal cancers. *Expert Opin Biol Ther* **4**: 1241–1250.
9. Yamamoto, M and Curiel, DT (2010). Current issues and future directions of oncolytic adenoviruses. *Mol Ther* **18**: 243–250.
10. Green, N and Seymour, L (2002). Adenoviral vectors: Systemic delivery and tumor targeting. *Cancer Gene Ther* **9**: 1036–1042.
11. Reid, T, Galanis, E, Abbruzzese, J, Sze, D, Andrews, J, Romel, L *et al.* (2001). Intra-arterial administration of a replication-selective adenovirus (dl1520) in patients with colorectal carcinoma metastatic to the liver: a phase I trial. *Gene Ther* **8**: 1618–1626.
12. Reid, T, Galanis, E, Abbruzzese, J, Sze, D, Wein, LM, Andrews, J *et al.* (2002). Hepatic arterial infusion of a replication-selective oncolytic adenovirus (dl1520): phase II viral, immunologic, and clinical endpoints. *Cancer Res* **62**: 6070–6079.
13. Mulvihill, S, Warren, R, Venook, A, Adler, A, Randlev, B, Heise, C *et al.* (2001). Safety and feasibility of injection with an E1B-55 kDa gene-deleted, replication-selective adenovirus (ONYX-015) into primary carcinomas of the pancreas: a phase I trial. *Gene Ther* **8**: 308–315.
14. Hecht, JR, Bedford, R, Abbruzzese, JL, Lahoti, S, Reid, TR, Soetikno, RM *et al.* (2003). A phase I/II trial of intratumoral endoscopic ultrasound injection of ONYX-015 with intravenous gemcitabine in unresectable pancreatic carcinoma. *Clin Cancer Res* **9**: 555–561.
15. Saukkonen, K and Hemminki, A (2004). Tissue-specific promoters for cancer gene therapy. *Expert Opin Biol Ther* **4**: 683–696.
16. Krasnykh, VN, Mikheeva, GV, Douglas, JT and Curiel, DT (1996). Generation of recombinant adenovirus vectors with modified fibers for altering viral tropism. *J Virol* **70**: 6839–6846.
17. Wu, H and Curiel, DT (2008). Fiber-modified adenoviruses for targeted gene therapy. *Methods Mol Biol* **434**: 113–132.
18. Bai, L and Morozov, AV (2010). Gene regulation by nucleosome positioning. *Trends Genet* **26**: 476–483.
19. Montecino, M, Stein, JL, Stein, GS, Lian, JB, van Wijnen, AJ, Cruzat, F *et al.* (2007). Nucleosome organization and targeting of SWI/SNF chromatin-remodeling complexes: contributions of the DNA sequence. *Biochem Cell Biol* **85**: 419–425.
20. Gutiérrez, J, Sierra, J, Medina, R, Puchi, M, Imschenetzky, M, van Wijnen, A *et al.* (2000). Interaction of CBF alpha/AML/PEBP2 alpha transcription factors with nucleosomes containing promoter sequences requires flexibility in the translational positioning of the histone octamer and exposure of the CBF alpha site. *Biochemistry* **39**: 13565–13574.
21. Gutiérrez, J, Paredes, R, Cruzat, F, Hill, DA, van Wijnen, AJ, Lian, JB *et al.* (2007). Chromatin remodeling by SWI/SNF results in nucleosome mobilization to preferential positions in the rat osteocalcin gene promoter. *J Biol Chem* **282**: 9445–9457.
22. Villagra, A, Cruzat, F, Carvallo, L, Paredes, R, Olate, J, van Wijnen, AJ *et al.* (2006). Chromatin remodeling and transcriptional activity of the bone-specific osteocalcin gene require CCAAT/enhancer-binding protein beta-dependent recruitment of SWI/SNF activity. *J Biol Chem* **281**: 22695–22706.
23. Moon, RT, Kohn, A, De Ferrari, GV and Kaykas, A (2004). Wnt and β-catenin signaling: diseases and therapies. *Nature Rev* **5**: 689–699.
24. Kolligs, FT, Bommer, G and Göke, B (2002). Wnt/beta-catenin/tcf signaling: a critical pathway in gastrointestinal tumorigenesis. *Digestion* **66**: 131–144.
25. Korinek, V, Barker, N, Morin, PJ, van Wichen, D, de Weger, R, Kinzler, KW *et al.* (1997). Constitutive transcriptional activation by a beta-catenin-Tcf complex in APC-/- colon carcinoma. *Science* **275**: 1784–1787.
26. Yu, J, Zhang, L, Hwang, PM, Kinzler, KW and Vogelstein, B (2001). PUMA induces the rapid apoptosis of colorectal cancer cells. *Mol Cell* **7**: 673–682.
27. Malerba, M, Nikolova, D, Cornelis, J and Iggo, R (2006). Targeting of autonomous parvoviruses to colon cancer by insertion of Tcf sites in the P4 promoter. *Cancer Gene Ther* **13**: 273–280.
28. Kuroda, T, Rabkin, SD and Martuza, RL (2006). Effective treatment of tumors with strong beta-catenin/T-cell factor activity by transcriptionally targeted oncolytic herpes simplex virus vector. *Cancer Res* **66**: 10127–10135.
29. Liu, X, Qian, Q, Xu, P, Wolf, F, Zhang, J, Zhang, D *et al.* (2011). A novel conditionally replicating "armed" adenovirus selectively targeting gastrointestinal tumors with aberrant wnt signaling. *Hum Gene Ther* **22**: 427–437.
30. Nuñez, F, Bravo, S, Cruzat, F, Montecino, M and De Ferrari, GV (2011). Wnt/β-catenin signaling enhances cyclooxygenase-2(COX2) transcriptional activity in gastric cancer cells. *PLoS ONE* **6**: e18562.
31. Fukui, H, Fujii, S, Takeda, J, Kayahara, T, Sekikawa, A, Nanakin, A *et al.* (2003). Expression of Reg 1α protein in human gastric cancers. *Digestion* **69**: 177–184.
32. Tanaka, H, Fukui, H, Fujii, S, Sekikawa, A, Yamagishi, H, Ichikawa, K *et al.* (2011). Immunohistochemical analysis of REG Ia expression in ulcerative colitis-associated neoplastic lesions. *Digestion* **83**: 204–209.
33. Zhou, L, Zhang, R, Wang, L, Shen, S, Okamoto, H, Sugawara, A *et al.* (2010). Upregulation of REG Ialpha accelerates tumor progression in pancreatic cancer with diabetes. *Int J Cancer* **127**: 1795–1803.
34. Cafferata, E, Maccio, D, Lopez, M, Viale, D, Carbone, C, Mazzolini, G *et al.* (2009). A novel A33 promoter based conditionally replicative adenovirus suppresses tumor growth and eradicates hepatic metastases in human colon cancer models. *Clin Cancer Res* **15**: 2037–2049.
35. Viale, DL, Cafferata, EG, Gould, D, Rotondaro, C, Chernajovsky, Y, Curiel, DT *et al.* (2013). Therapeutic improvement of a stroma-targeted CRAd by incorporating motives responsive to melanoma microenvironment. *J Invest Dermatol* (in press).
36. Sakakibara, Y, Irie, T, Suzuki, Y, Yamashita, R, Wakaguri, H, Kanai, A *et al.* (2007). Intrinsic promoter activities of primary DNA sequences in the human genome. *DNA Res* **14**: 71–77.
37. Stein, GS, van Wijnen, AJ, Imbalzano, AN, Montecino, M, Zaidi, SK, Lian, JB *et al.* (2010). Architectural genetic and epigenetic control of regulatory networks: compartmentalizing machinery for transcription and chromatin remodeling in nuclear microenvironments. *Crit Rev Eukaryot Gene Expr* **20**: 149–155.
38. Vane, JR, Bakhle, YS and Botting, RM (1998). Cyclooxygenases 1 and 2. *Annu Rev Pharmacol Toxicol* **38**: 97–120.
39. Modlich, U, Pugh, CW and Bicknell, R (2000). Increasing endothelial cell specific expression by the use of heterologous hypoxic and cytokine-inducible enhancers. *Gene Ther* **7**: 896–902.
40. Policastro, LL, Ibañez, IL, Durán, HA, Soria, G, Gottifredi, V and Podhajcer, OL (2009). Suppression of cancer growth by nonviral gene therapy based on a novel reactive oxygen species-responsive promoter. *Mol Ther* **17**: 1355–1364.
41. Zaretsky, JZ, Barnea, I, Aylon, Y, Gorivodsky, M, Wreschner, DH and Keydar, I (2006). MUC1 gene overexpressed in breast cancer: structure and transcriptional activity of the MUC1 promoter and role of estrogen receptor alpha (ERalpha) in regulation of the MUC1 gene expression. *Mol Cancer* **5**: 57.
42. Lee, CY, Bu, LX, DeBenedetti, A, Williams, BJ, Rennie, PS and Jia, WW (2010). Transcriptional and translational dual-regulated oncolytic herpes simplex virus type 1 for targeting prostate tumors. *Mol Ther* **18**: 929–935.
43. Yochum, GS (2011). Multiple Wnt/ß-catenin responsive enhancers align with the MYC promoter through long-range chromatin loops. *PLoS ONE* **6**: e18966.
44. Morin, PJ, Sparks, AB, Korinek, V, Barker, N, Clevers, H, Vogelstein, B *et al.* (1997). Activation of beta-catenin-Tcf signaling in colon cancer by mutations in beta-catenin or APC. *Science* **275**: 1787–1790.
45. Lopez, MV, Rivera, AA, Viale, DL, Benedetti, L, Cuneo, N, Kimball, KJ *et al.* (2012). A tumor-stroma targeted oncolytic adenovirus replicated in human ovary cancer samples and inhibited growth of disseminated solid tumors in mice. *Mol Ther* **20**: 2222–2233.
46. Paredes, R, Arriagada, G, Cruzat, F, Villagra, A, Olate, J, Zaidi, K *et al.* (2004). Bone-specific transcription factor Runx2 interacts with the 1alpha,25-dihydroxyvitamin D3 receptor to up-regulate rat osteocalcin gene expression in osteoblastic cells. *Mol Cell Biol* **24**: 8847–8861.